STM study of C_2H_2 adsorption on Si(001)

L. Li, C. Tindall, O. Takaoka, Y. Hasegawa, and T. Sakurai
Institute for Materials Research, Sendai 980-77, Japan
(Received 11 November 1996; revised manuscript received 24 March 1997)

We present here a scanning tunneling microscope study of the initial bonding structure and subsequent reaction mechanism of C_2H_2 with the Si(001) surface. Upon exposure of the sample at room temperature to 0.2 L of C_2H_2 (approximately 20% coverage) adsorption of the molecule on alternate dimer pairs is observed, leading to either a local 2×2 or $c(2\times4)$ structure. In the filled-state image, a local minimum is observed in the center of the reacted dimer pairs, while the unreacted dimer pairs maintain the normal bean-shaped contour of the clean surface. The molecule forms an overlayer with either local 2×2 or $c(4\times2)$ order, leading to a saturation coverage of 0.5 monolayers. Upon annealing the substrate at 775 K the surface becomes disordered and the steps are no longer visible. After further annealing at 875 K, SiC clusters are formed and the 2×1 structure is again seen between the clusters. For a starting coverage of 20%, annealing to higher temperatures around 1100 K leads to pinning of the step movement by the SiC clusters. For a starting coverage of 0.5 monolayer, annealing at 1100 K results in faceting of the surface. Further annealing at 1275 K creates anisotropic facets that are oriented along the $[\bar{1}10]$ direction with a typical aspect ratio of approximately 4 to 5. These facets act as nucleation sites for subsequent carbonization and SiC growth. [S0163-1829(97)05032-7]

I. INTRODUCTION

SiC has recently attracted increasing attention because of its potential applications for high-power, high-temperature electronic devices,[1] short-wavelength light-emitting diodes (LED's),[2] and as a substrate for the growth of nitrides, most notably GaN. SiC exists in 250 different polytypes, the structure of which is determined by the Si/C layer stacking sequence.[3] Each of these polytypes has slightly different electronic properties. Thus a polytype can be chosen that has the best properties for the desired application. For example, the most common polytype 6 hexagonal–SiC is of interest for short-wavelength (blue) LED's because of its wide band gap. Another polytype that has potential device applications is cubic silicon carbide 3 cubic–SiC. Because of its high breakdown field, relatively wide band gap (compared to Si), and excellent thermal conductivity, it is a candidate as a material for high-temperature, high-power electronics. This increased interest in SiC for device applications has been stimulated by recent progress in single-crystal SiC growth techniques.[2] However, the cost of single-crystal SiC material remains very high.[4]

For this reason, heteroepitaxial growth of $3C$-SiC on Si surfaces has been studied by many different groups.[5–7] Thin-film growth typically begins with carbonization of the Si(001) surface using various carbon sources ranging from small hydrocarbons, typically either C_2H_2 or C_2H_4, to carbon particles obtained from the evaporation of graphite.[8] There have also been a number of studies of the fundamental reaction mechanism of these molecules with the Si(001) surface.[9–11] However, in the case of C_2H_2, the exact nature of the initial bonding geometry of the molecule with the Si(001) surface is still a matter of discussion, as well as the detailed structure of the overlayer. In addition, to date there is no scanning tunneling microscope (STM) study of the fundamental reaction mechanism and the initial growth morphology of the SiC layer.

II. EXPERIMENTAL DETAILS

The experiments were carried out in an UHV chamber containing a STM equipped with a low-energy electron diffraction (LEED) and field-ion microscope that is used to monitor and fabricate the tip. The base pressure was approximately 5×10^{-11} torr. The details of the chamber design are described elsewhere.[12] The silicon sample p-type [Si(001)] was annealed to 1200 °C to prepare clean substrates. The acetelyne (99.8% purity) was used without further purification. The chemical was dosed onto the sample from the chamber background pressure. The dosage was estimated using the uncorrected ion gauge reading.

III. RESULTS AND DISCUSSION

A. Adsorption at 300 K

Figure 1(a) shows a filled-state image of the surface after adsorption of 0.2 L of C_2H_2 at 300 K. Most of the surface dimers display the normal ''bean'' shape, which is characteristic of clean, unreacted dimers on Si(001) in the filled-state image.[13] On the other hand, there are also features that are imaged as dark spots in the dimer rows. These features, unlike the clean dimers, have an additional local minimum that is seen in the center of the dimer row. Since this secondary minimum is not seen in the filled-state image for the clean surface, we conclude that the depressions correspond to reacted dimer sites. Figure 1(b) shows a smaller area of the surface with a line plot that shows the apparent height difference between the reacted and unreacted sites. Here the relative height variation parallel to the direction of the dimer row is shown. As can be seen from the scale in the figure, the apparent height difference between the reacted and unreacted sites is approximately 0.7 ± 0.1 Å. This is about half the height of a single step on the Si(001) surface.[14] Figure 1(c) illustrates the secondary minimum seen in the reacted sites. The line plot is perpendicular to the dimer row and crosses

0163-1829/97/56(8)/4648(8)/$10.00 © 1997 The American Physical Society

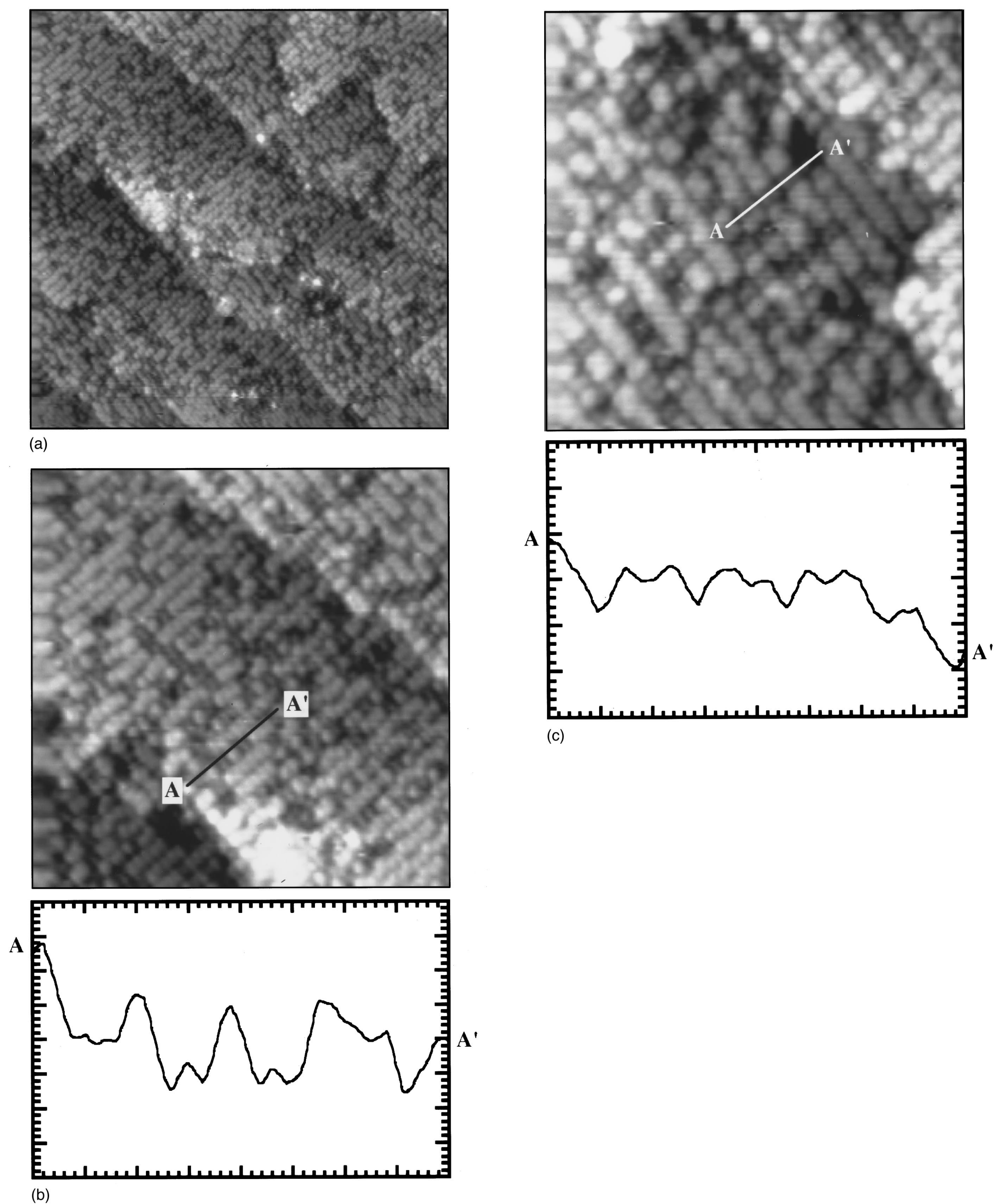

FIG. 1. (a) Filled-state image of the Si(100) surface after exposure to 0.2 L of C_2H_2. Reacted dimers are imaged as depressions in the dimer row. The sample bias is -2.0 V. The image size is 300×300 Å^2. (b) Close-up image taken from (a). The line plot shows the apparent height difference across two reacted dimers and two unreacted dimers parallel to the dimer row. The image size is 150×150 Å^2. (c) Close-up image taken from (a). The line plot shows the apparent height difference across three reacted dimers, showing the secondary minimum at the center of the reacted dimer. Note that this minimum is not observed on clean, unreacted dimers. The image size is 150 $\times150$ Å^2.

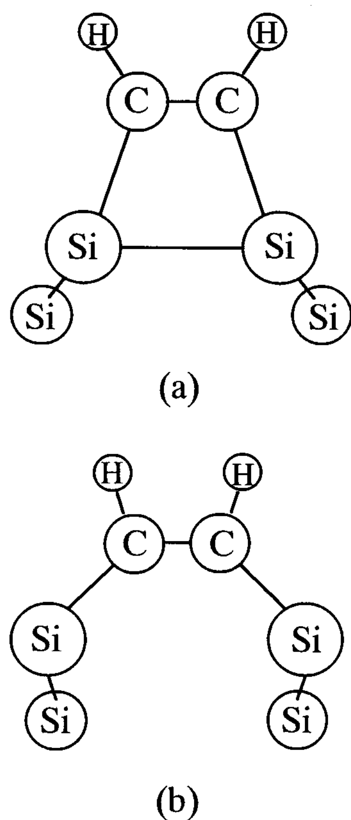

FIG. 2. Model for the initial adsorption geometry of C_2H_2 on Si(100) proposed in previous studies: (a) the dimerized model in which there is no cleavage of the Si-Si dimer bond and (b) the dimer cleaved model.

three reacted sites that are adjacent to one another in different dimer rows. As one moves from A to A' a relatively deep minimum is encountered. This deep minimum is located between the dimer rows. Next, two maxima separated by a shallower minimum are seen. This is again followed by a deeper minimum that is located between the dimer rows. We now proceed with a summary of previous work that has been done on this system and a discussion of the origin of this secondary minimum in the image in terms of the bonding geometry of the molecule.

In previous studies, an initial bonding geometry in which the molecule bonds nondissociatively and symmetrically to the dimer pair with the C-C bond parallel to the surface as shown in Fig. 2 has been proposed.[9,11,15,16] The primary experimental evidence for molecular adsorption is provided by the high-resolution electron-energy-loss spectroscopy (HREELS) vibrational spectrum. However, the data are open to interpretation and there is some disagreement on the correct peak assignments. Because of this, some controversy remains over the exact nature of the initial bonding geometry. It is generally agreed that the primary adsorption pathway for C_2H_2 is nondissociative adsorption. Moreover, both theoretical and experimental studies indicate that the molecule bonds across the Si-Si dimer with the C-C bond parallel to the surface. However, a point of contention remains over whether or not the underlying Si-Si dimer bond cleaves upon adsorption. Both the experimental studies as well as the theoretical calculations are divided on this issue. Of particular relevance to our discussion is the calculation of Imamura *et al.* They have calculated the charge density of C_2H_2 bonded to the Si(001)2×1 surface.[15] In both configurations, i.e., with and without Si-Si dimer bond cleavage, the charge density exhibits a minimum between the two hydrogen atoms. Thus, as the STM tip passes over a reacted dimer site, in order to maintain a constant tunneling current, it will have to move closer to the surface causing the center of the dimer to appear lower. As discussed above, Fig. 1(c) shows a smaller scale image of the surface in which the secondary minimum on the reacted sites is clearly visible. The line plot shows the apparent height difference as one moves perpendicularly across three reacted dimers. In each case, a distinct doubly peaked structure is seen. Thus the existence of this minimum in the center of the dimer row in the filled-state image clearly identifies this as a reacted dimer. Furthermore, this image is consistent with the basic features of the previously proposed adsorption geometry, that is to say, the molecule bonds across the silicon dimer, with no adsorption being observed between the dimer rows. The apparent depth of the central minimum observed in the reacted dimers is 0.3 ± 0.1 Å. This can be compared with the calculated variation in the charge density of the reacted dimers. For the dimerized model (i.e., the underlying Si-Si dimer bond is still intact) the depth of this minimum is approximately 0.5 Å. In the case of the dimer-cleaved configuration it is about 1.1 Å.[15] This would seem to favor the dimerized configuration over the dimer cleaved arrangement.

A second relevant point concerns the calculated charge-density distribution of the dimer-cleaved configuration. With the C_2H_2 bonded in this way, there are two lobes arising from dangling-bond states, which extend between the first-layer Si atoms in adjacent dimer rows. These dangling-bond states are absent in the dimerized geometry.[15] Thus the existence or lack of these dangling-bond states gives information on whether or not the Si-Si dimer bond is cleaved. We can determine from our STM images whether or not these dangling-bond states are present by measuring the depth of the minimum between the dimer rows. The depth of the minimum between dimer rows on clean Si(001) was measured by Hamers and co-workers.[13,17] They concluded that a depth of approximately 0.5 Å was most consistent with their STM images. We obtained a somewhat larger value from our images: 0.7 ± 0.1 Å. The discrepancy may be due to the fact that we are measuring the value directly from the STM image, whereas Hamers and co-workers calculated the corrugation profile that fit best overall to their STM image. From our STM image the apparent depth of the minimum between reacted dimers on adjacent dimer rows is 0.6 ± 0.1 Å. The anticipated depth of the minimum between two reacted dimers for the dimer-cleaved geometry is approximately 0.4 Å. That of the dimerized configuration is much deeper. No depth can be estimated from the calculation since the line indicating the smallest calculated value of constant charge density does not extend across the dimer row. Therefore, for the dimerized geometry, the depth of the minimum between reacted dimer sites should be larger than 0.4 Å, but less than or equal to 0.7 Å. Our measured value is less than that of the clean surface. However, it still falls within the experimental error of the clean surface measurement. Therefore, the STM image does not provide any indication that there are dangling-bond states present at the reacted dimer

FIG. 3. Filled-state image of the Si(100) surface after exposure to 2 L of C_2H_2. This exposure resulted in saturation coverage and produced an ordered 2×2 overlayer. The image size is 300 $\times300$ Å^2. The sample bias is -2.4 V.

sites. To summarize, because of the agreement in the measured depth of the central minimum with the calculated value and the absence of Si dangling-bond states on the reacted dimers, the STM data are more consistent with the dimerized model than with the dimer-cleaved model.

Figure 3 is an image of the surface obtained after exposure to 2 L of C_2H_2 at 300 K. Because of its two π bonds, this molecule is very reactive towards Si(001). A 2-L exposure saturates the surface with C_2H_2. Exposures of up to 100 L failed to produce any increase in the surface coverage beyond that seen at 2 L of exposure. From this image, it can be seen that the C_2H_2 adsorbs on alternate dimers. Thus the C_2H_2 overlayer exhibits a either local 2×2 or $c(2\times4)$ structure, depending on whether the C_2H_2 adsorbed on adjacent rows is in phase or out of phase. Thus the saturation coverage is 0.5 monolayer. This result contrasts with a previous temperature-programmed desorption (TPD) study in which the saturation coverage was determined to be approximately 0.83 monolayer. The authors of that study concluded that C_2H_2 molecules adsorb on every Si dimer pair and that saturation coverage was thus one monolayer, i.e., one C atom for every Si atom. They attributed the discrepancy between full coverage and their measured value for the actual coverage to a high density of defects at which they anticipated no C_2H_2 adsorption.[10]

Previous LEED studies have indicated that the 2×1 pattern of the clean reconstructed surface is retained after adsorption of the C_2H_2. However, an apparent 2×1 LEED pattern could still be consistent with a 2×2 overlayer if the scattering cross section of the C_2H_2 is relatively small. If this were the case, one would expect the incoming electrons to still ''see'' the Si(001)2×1 surface and thus the original 2 $\times1$ pattern would still be visible. Moreover, the existence of the 2×2 overlayer would not create any additional spots in the LEED pattern. Therefore, in the absence of a detailed

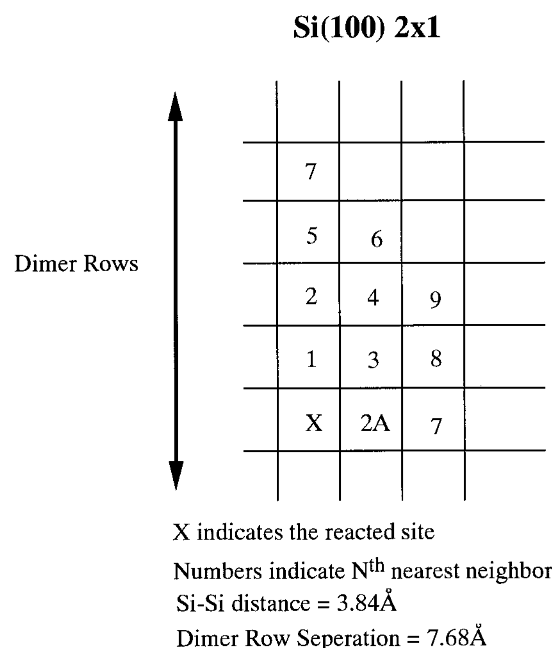

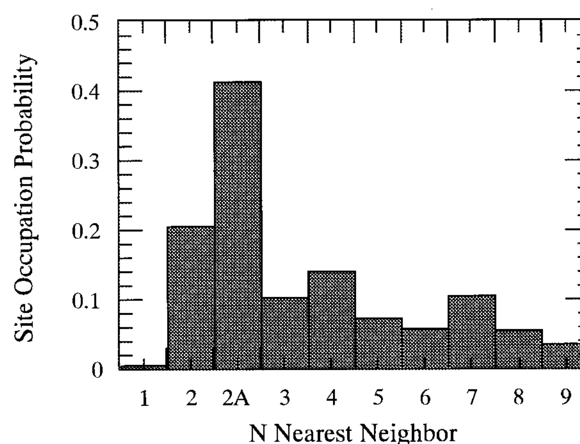

FIG. 4. Plot of the site occupation probability for the nearest neighbor to the ninth nearest neighbor. The plot was obtained from STM images of the Si(100) after exposure to 0.2 L of C_2H_2 at 300 K. Reacted sites were chosen and the occupation of neighboring sites was then tabulated.

study of spot intensities, differentiation between a 2×2 overlayer structure and a 2×1 structure would be difficult. In addition, because the domain size of the overlayer is fairly small, i.e., less than the typical 100 Å coherence length of the LEED electrons, the existence of the overlayer should lead to an increase in the background scattering, which was observed.[11]

The lack of adsorption on nearest-neighbor sites is shown clearly in the plot of site occupation probability for various neighboring sites for a 0.2-L dose shown in Fig. 4. For an ideal $p(2\times2)$ structure, sites 2, 2A, 4, 7, and 9 should be occupied with a probability of one. The other sites should be unoccupied. For a perfect $c(4\times2)$ structure sites 2, 3, 6, 7, and 9 should be occupied, while the rest are unoccupied. The graph shows that only a very small number of nearest-neighbor sites are occupied. The lack of adsorption on nearest-neighbor sites implies some sort of repulsive interac-

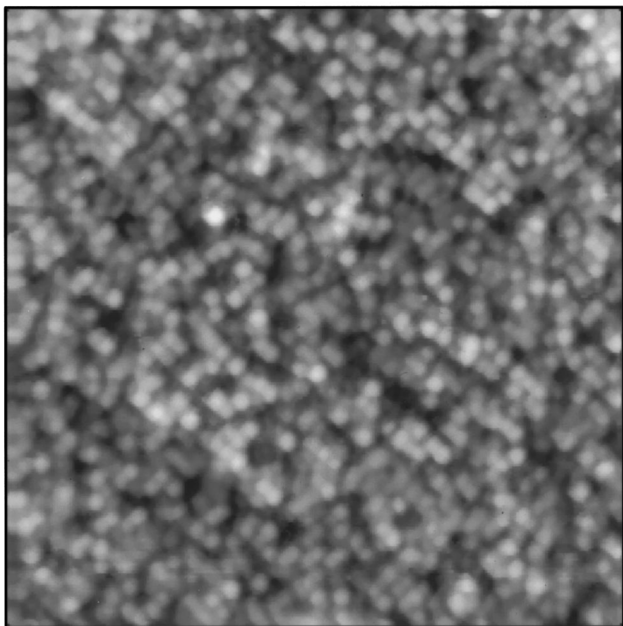

FIG. 5. Filled-state image of the Si(100) surface after exposure to 0.2 L of C_2H_2 at 300 K and subsequent annealing at 775 K for 5 min. The image size is 225×225 Å^2. The sample bias is −1.8 V.

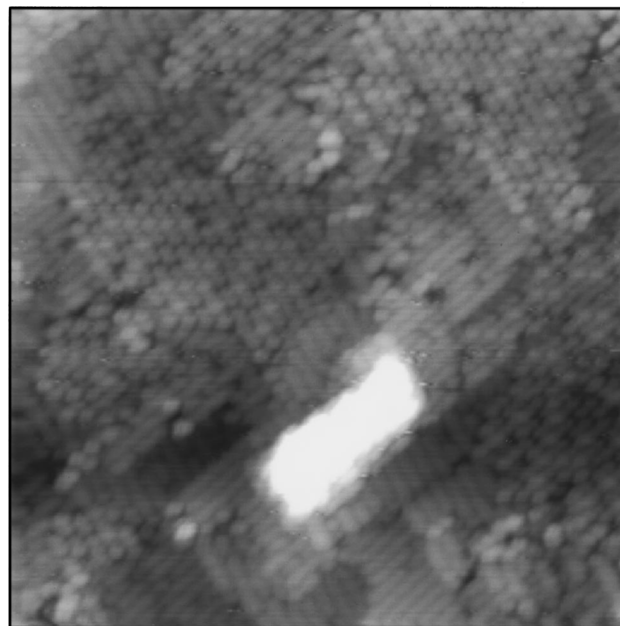

FIG. 6. Filled-state image of the Si(100) surface after exposure to 0.2 L of C_2H_2 at 300 K and subsequent annealing at 950 K for 5 min. Annealing at this temperature resulted in the formation of SiC islands, one of which is shown here. The image size is 300 ×300 Å^2. The sample bias is −2.0 V.

tion between the C_2H_2 molecules. In the following paragraph we discuss a possible mechanism for this interaction.

The adsorption kinetics of C_2H_2 on Si(001) suggest that the adsorption takes place via a mobile precursor mechanism.[10] The electron-structure calculation done by Imamura *et al.* also shows that the C-H bonds in the adsorbed complex are quite polar. Although the gas-phase C_2H_2 molecule is symmetric and thus has no permanent dipole moment, the electronegativity of C in acetylene is relatively high because of the large percentage of *s* character of the molecular orbitals.[18] Therefore, the C-H bonds in gas-phase acetylene are also quite polar. Thus the C_2H_2 molecule that is in the process of adsorbing could interact with one that is already adsorbed in a way that prevents it from adsorbing on nearest-neighbor sites. In addition, if upon entering the precursor state the molecule deforms slightly this should enhance the strength of the interaction by giving the adsorbing C_2H_2 a macroscopic dipole moment. Finally, a recent STM study of C_2H_2 adsorption on Si(001) has shown that ethylene also adsorbs on alternate dimers.[19] A dipole interaction could also be the cause of the ordering of that molecule on Si(001).

B. Surface reaction mechanism

In order to study the surface reaction mechanism, we started by annealing a Si(001) surface that had been exposed to 0.2 L of C_2H_2 at 300 K. Annealing this surface to 575 K for 5 min resulted in very little change of the surface morphology. Only a slight amount of disordering was noted. However, as seen in Fig. 5, annealing at 775 K for 5 min resulted in a very disordered surface. Large area scans (1125×1125 Å^2) did not show any well-defined step structure. There is a strong Si-H stretching mode visible at 265 meV in the HREELS spectrum after annealing the C_2H_2 exposed surface at this temperature.[9,11] The C-H stretching mode at 373 meV is also seen in the vibrational spectrum. Thus there is C-H present on the surface as well. At this temperature the 86-meV peak due to C-C stretching broadened and developed a long tail. This most likely indicated the formation of additional Si-C bonds on the surface since a 100-meV loss peak is characteristic of the Si-C stretching mode.[11] In summary, at this point in the reaction, there is some dehydrogenation of the C_2H_2 to produce Si-H while the number of Si-C bonds is increasing. Thus we conclude that the surface atoms have become mobile enough to begin to form small clusters of Si, C, and H.

Despite the lack of order seen after annealing at 775 K, further annealing for 5 min at 950 K resulted in the formation of small clusters on the surface, and clean silicon was again visible between the clusters. In general the clusters tend to nucleate at step edges on terraces with the dimer rows perpendicular to the step edge, i.e., type ‘‘*B*’’ steps. Moreover, areas of silicon depletion immediately surrounding the clusters were visible in the images, as shown in Fig. 6. The depletion of silicon next to the cluster is seen from the fact that in this image, five layers of silicon have become visible. Furthermore, the silicon immediately surrounding the cluster is relatively defect free compared with the rest of the surface. This suggests that the layers of silicon that previously covered these layers have been removed and incorporated into the cluster. Another point of interest in this image is the very high missing dimer defect density that is seen in the silicon surface relatively far from the cluster. The missing dimer defects primarily consist of a single missing dimer pair. However, upon closer examination of the areas of high defect density, in addition to the missing dimer defects that are imaged as dark spots, there are also bright spots visible in the dimer rows. Taken together with the missing dimer defects, the bright and dark features form a very well-ordered $c(4$

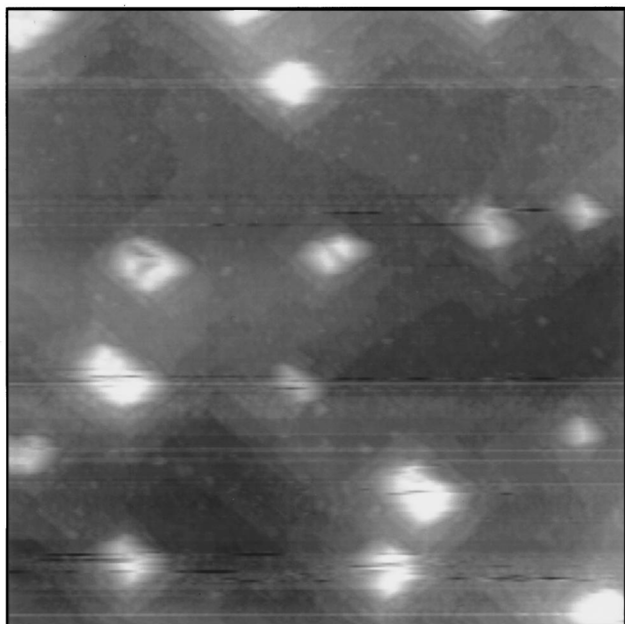

FIG. 7. Filled-state image of the Si(100) surface after exposure to 0.2 L of C_2H_2 at 300 K and subsequent annealing at 1275 K for 5 min. The SiC islands formed act as pinning centers, restricting the step movement. The image size is 750×750 Å^2. The sample bias is -2.5 V.

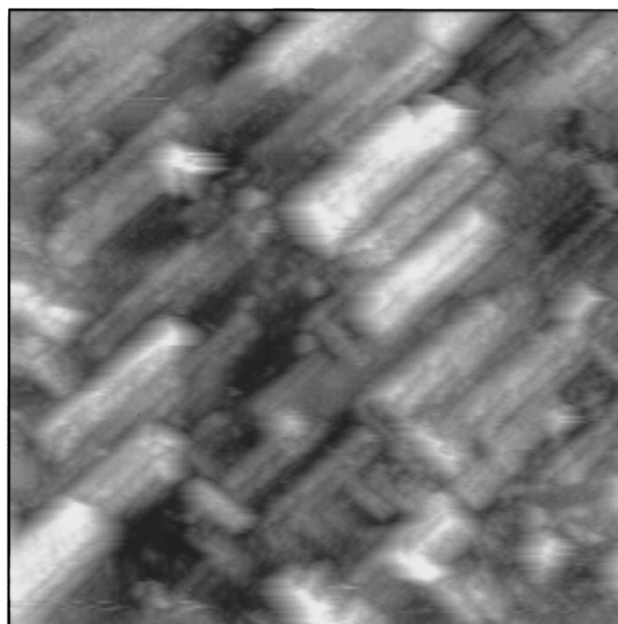

FIG. 8. Filled-state image of the Si(100) surface after exposure to 2 L (saturation coverage) of C_2H_2 at 300 K and subsequent annealing at 1275 K for 5 min. Well-defined facets are formed on the surface that act as nucleation sites for further SiC growth. The image size is 1125×1125 Å^2. The sample bias is -2.5 V.

$\times4$) structure. This is know to be a metastable phase of the Si(001) surface and can be formed in a number of different ways: by exposure to hydrogen or ethylene or simply by annealing within the appropriate temperature range.[20,21] The bright spots in the image are Si ad-dimers, which are know to be present in the $c(4\times4)$ phase.

Annealing again at 1275 K for 5 min resulted in more step movement, with the step movement being pinned by the clusters formed on the surface. The predominant shape of the clusters was rectangular. Figure 7 shows a typical image of the surface after annealing at this temperature. Reacting a small amount of C_2H_2 with the surface leads to SiC clusters rather than the more dramatic faceting that is obtained when one starts with higher coverages.

Figure 8 shows an image of the Si(001) surface that was first exposed to 2 L of C_2H_2- (saturation dose) at 300 K and subsequently annealed at 1275 K for 1 min. The intermediate steps of the reaction obtained by annealing below 900 K are very similar to those obtained at lower coverages. However, at high temperatures, formation of SiC beginning with saturation coverage of C_2H_2 results in pronounced faceting of the surface rather than simply the formation of discrete SiC islands that are formed if one starts with lower coverages. If one starts with saturation coverage, the step structure of the original surface is obliterated by the faceting induced by the SiC growth. A substantial amount of mass movement has taken place during the creation of the facets. The faceting is strongly anisotropic, producing rectangularly shaped surface structures with an approximate aspect ratio (ratio of the length to the width) of about 4:1. The axes of the facets are oriented in the [$\bar{1}$10] and [110] directions. The vast majority of the facets are oriented with their major axes parallel to each other in the [$\bar{1}$10] direction, but there are also smaller facets visible in the image that have their major axes oriented perpendicular to that of the larger facets. The angle of the facets was measured using the apparent height difference from the base to the top of the facets. The angle was somewhat dependent on the size of the facet, with the larger facets having a steeper slope. The angle of the facets varied from approximately 10.4° to 24.5° away from the [001] direction towards [111]. The smallest facets had angles of approximately 10°–11°, suggesting an approximately [118] orientation. The medium size facets have angles of 14°–16°, indicating an orientation of [116] to [115]. The angle of the large facets was measured to be between 18.5° and 19.5°, suggesting that these expose the [114] faces.[23] Finally, annealing at temperatures above 1325 K destroys the facets and again results in a disordered surface.

The origin of the faceting of the Si(100) surface upon reaction with carbon to form SiC was discussed by Kitabatake, Deguchi, and Hirao. The model they proposed is shown in Fig. 9. Their quasidynamic calculation qualitatively describes the structures that form after this reaction takes place.[5] Their model initially begins with a 1×1 silicon sur-

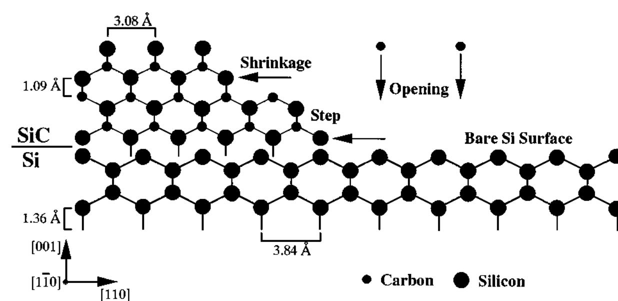

FIG. 9. Schematic of the SiC on Si growth model proposed in Ref. 5.

face on top of which are placed one *C* atom for every Si atom. As the temperature is increased, shrinkage occurs along the $[1\bar{1}0]$ direction due to the large lattice mismatch (20%) between SiC and Si. In addition, there is a significant amount of C penetration into the Si lattice. As can be seen in the figure, the shrinkage of the SiC lattice in the $[1\bar{1}0]$ direction produces facets similar to those seen in the STM image. However, this model only describes qualitatively how the faceting developed, thus no comparison with our measurement is possible. Our measurement of the angle of facets as a function of the facet size provides quantitative information of how the facets evolve, which can be used to guide future theoretical work.

Since, as discussed in the Introduction, there is a great deal of technological interest in growing SiC thin films on silicon substrates, the next logical step in our study is to grow a thicker layer of SiC on the surface and follow the evolution of the surface morphology. For the purpose of growth of a thicker layer, repeated cycles of the following procedure were used. First the clean surface was saturated with C_2H_2 and annealed in order to obtain the faceted surface shown in Fig. 8. This faceted surface was then dosed with a relatively large dose (20 L) of C_2H_2. This was followed by annealing the dosed, faceted surface at 1275 K in a Si flux for several minutes. The silicon flux was obtained by evaporating silicon from a thin slab of silicon placed near the sample. Following the silicon flux annealing step, the sample was further annealed at 1330 K for one more minute without the Si flux to evaporate excess silicon from the surface. The resulting surface is shown in Fig. 10. The further growth and ordering of the SiC facets is evident. At this stage, it was possible to image the top of the facets with atomic resolution. They exhibited 2×3 reconstruction, which is a typical surface phase of the silicon-rich, 3*C*-SiC(001) surface.[22]

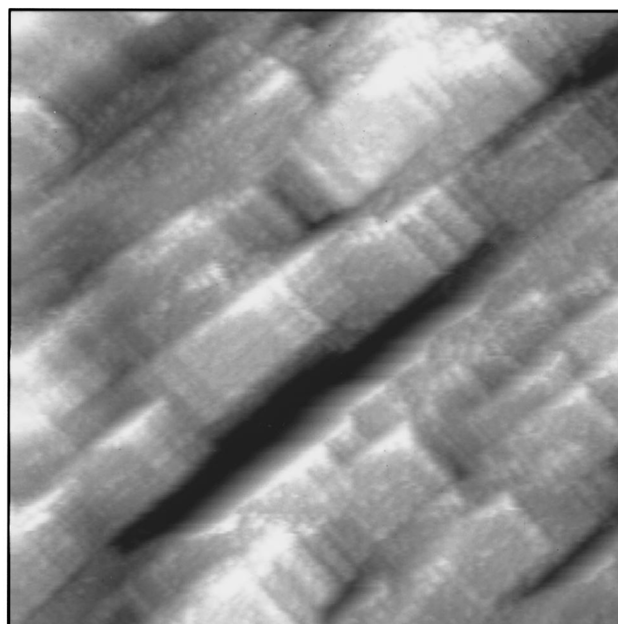

FIG. 10. Filled-state image of the Si(100) surface after several cycles exposure to 20 L of C_2H_2 at 300 K and subsequent annealing at 1275 K for 3 min in a silicon flux. The silicon flux was then turned off and the sample was annealed for one more minute at 1330 K. The image shows the additional growth of SiC in well-defined crystallites. Atomically resolved images of the top of the crystallites show that the surface has the 2×3 structure that is characteristic of the 3*C*-SiC(0001) surface. The image size is 1125 $\times1125$ Å^2. The sample bias is -2.5 V.

IV. CONCLUSIONS

We have presented here a STM study of the initial bonding structures and subsequent reaction mechanism of C_2H_2 with the Si(001) surface. Our STM images are consistent with the initial bonding geometry proposed in previous studies, specifically that the C_2H_2 molecule bonds across the silicon dimer, with no adsorption taking place inbetween the dimer rows. Furthermore, the STM data provide evidence to help resolve the issue of whether or not the underlying Si-Si dimer bond is cleaved. Our STM data are consistent with the dimerized model in which the Si-Si dimer bond remains intact. The overall structure of the adsorbate overlayer is locally 2×2 or $c(4\times2)$ rather than 2×1 as proposed in previous studies. Thus saturation coverage of C_2H_2 on this surface is 0.5 monolayer rather than 1 monolayer as previously suggested. Since C_2H_2 adsorption on this surface is known to take place via a mobile precursor mechanism, a possible cause for the formation of the 2×2 $[c(4\times2)]$ overlayer is a dipole-dipole interaction between the molecules during adsorption. The morphology obtained during the course of the reaction of the surface with C_2H_2 has been investigated. Annealing submonolayer coverages of the molecule first results in a disordered phase. This is followed by the creation of SiC clusters with a restoration of the Si(001)2×1 structure next to the clusters. The metastable $c(4\times4)$ Si(001) structure is formed between the clusters. At higher temperatures the SiC clusters pin the step movement. Annealing the saturated surface results in the formation of oriented, rectangular facets on the surface with an aspect ratio (length to width) of approximately 4. These facets act as nucleation sites for further SiC growth. Subsequent SiC growth using repeated cycles of adsorption followed by annealing in a silicon flux resulted in the growth of larger SiC crystals that exhibited the 2×3 surface reconstruction typical of the 3*C*-SiC polytype.

[1] H. Okumura *et al.*, J. Appl. Phys. **61**, 1134 (1987).

[2] J. R. Waldrop and R. W. Grant, Appl. Phys. Lett. **62**, 2685 (1993).

[3] O. Madelung, in *Semiconductors*, edited by O. Madelung, Landolt-Börnstein, New Series, Group III, Vol. 22a (Springer-Verlag, Berlin, 1987), p. 43.

[4] Cree Research Company, Raleigh, NC.

[5] M. Kitabatake, M. Deguchi, and T. Hirao, J. Appl. Phys. **74**, 4438 (1993).

[6] T. Yoshinobu, H. Mitsui, I. Izumikawa, T. Fuyuki, and H. Matsunami, Appl. Phys. Lett. **60**, 824 (1992).

[7] S. Hara, T. Megura, Y. Aoyagi, M. Kawai, S. Misawa, E. Sa-

kuma, and S. Yoshida, Thin Solid Films **225**, 240 (1993).
[8] I. Kusunoki, M. Hiroi, T. Sato, Y. Igari, and S. Tomoda, Appl. Surf. Sci. **45**, 171 (1990).
[9] C. Huang, W. Widdra, X. S. Wang, and W. H. Weinberg, J. Vac. Sci. Technol. A **11**, 2250 (1993).
[10] P. A. Taylor *et al.*, J. Am. Chem. Soc. **114**, 6754 (1992).
[11] M. Nishijima, J. Yoshinobu, H. Tsuda, and M. Onchi, Surf. Sci. **192**, 383 (1987).
[12] T. Sakurai *et al.*, Prog. Surf. Sci. **33**, 3 (1990).
[13] R. J. Hamers, R. M. Tromp, and J. E. Demuth, Phys. Rev. B **34**, 5343 (1986).
[14] H. Henzler and W. Ranke, in *Physics of Solid Surfaces*, edited by G. Chiarotti, Landolt-Börnstein, New Series, Group III, Vol. 24a (Springer-Verlag, Berlin, 1993), p. 284ff.
[15] Y. Imamura, Y. Morikawa, T. Yamasaki, and H. Nakatsuji, Surf. Sci. Lett. **341**, L1091 (1995).
[16] C. S. Carmer, B. Weiner, and M. Frenklach, J. Chem. Phys. **99**, 1356 (1993).
[17] R. M. Tromp, R. J. Hamers, and J. E. Demuth, Phys. Rev. Lett. **55**, 1303 (1985).
[18] S. Ege, *Organic Chemistry*, 2nd ed. (Heath & Co., Lexington, MA, 1989), p. 56.
[19] A. J. Mayne, A. R. Avery, J. Knall, T. S. Jones, G. A. D. Briggs, and W. H. Weinberg, Surf. Sci. **284**, 247 (1993).
[20] R. I. G. Uhrberg, J. E. Northrup, D. K. Biegelsen, R. D. Bringans, and L.-E. Swartz, Phys. Rev. B **46**, 10 251 (1992).
[21] T. Takaoka, T. Takagaki, Y. Igari, and I. Kusunoki, Surf. Sci. **347**, 105 (1996).
[22] S. Hara, S. Misawa, and S. Yoshida, Phys. Rev. B **50**, 4548 (1994).
[23] S. C. Erwin, A. A. Baski, and L. J. Whiteman, Phys. Rev. Lett. **77**, 687 (1996).